

Insights into aqueous carbofuran removal by modified and non-modified rice husk biochars

S.S. Mayakaduwa¹ · Indika Herath¹ · Yong Sik Ok² · Dinesh Mohan³ · Meththika Vithanage¹

Received: 22 December 2015 / Accepted: 4 August 2016 / Published online: 23 August 2016
© Springer-Verlag Berlin Heidelberg 2016

Abstract Biochar has been considered as a potential sorbent for removal of frequently detected pesticides in water. In the present study, modified and non-modified rice husk biochars were used for aqueous carbofuran removal. Rice husk biochars were produced at 300, 500, and 700 °C in slow pyrolysis and further exposed to steam activation. Biochars were physicochemically characterized using proximate, ultimate, FTIR methods and used to examine equilibrium and dynamic adsorption of carbofuran. Increasing pyrolysis temperature led to a decrease of biochar yield and increase of porosity, surface area, and adsorption capacities which were further enhanced by steam activation. Carbofuran adsorption was pH-dependant, and the maximum (161 mg g⁻¹) occurred in the vicinity of pH 5, on steam-activated biochar produced at 700 °C. Freundlich model best fitted the sorption equilibrium data. Both chemisorption and physisorption interactions on heterogeneous adsorbent surface may involve in carbofuran adsorption. Langmuir kinetics could be applied to describe carbofuran adsorption in a fixed bed. A higher carbofuran volume was treated in a column bed by a steam-activated biochar versus non-activated biochars. Overall, steam-

activated rice husk biochar can be highlighted as a promising low-cost sustainable material for aqueous carbofuran removal.

Keywords Agricultural by-product · Dynamic adsorption · Pesticide · Pyrolysis · Activated carbon · Steam activation

Introduction

The rapid development of agriculture has led to the increased use of pesticides during the last decades. As a result, pesticide residues are ubiquitous in both surface and groundwater (Salman and Hameed 2010) posing hazard to living organisms. Carbofuran (2,3-dihydro-2,2-dimethyl-7-benzofuranyl-N-methylcarbamate) is a highly effective pesticide of the carbamate group, used against a wide range of insects adversely affecting a variety of fruit and vegetable crops. Further, it is soluble in water and highly mobile in soil, thereby having a high potential for contamination of surface water as well as groundwater (Remya and Lin 2011). There are considerable risks associated with the presence of carbofuran in drinking water, since it may cause irreversible neurological damages to living organisms. The half-life of carbofuran in water is variable which ranged from 690 days at pH 5 to 7 days at pH 9 (Makehelwala et al. 2012). World Health Organization (WHO) admits a maximum limit of 3 µg L⁻¹ (WHO 2006) while the EPA specifies an acceptable limit of 40 µg L⁻¹ in drinking water (DeZuane 1997).

Average annual usage of carbofuran was 2.7 to 4 million kg in the USA, and Kenya imported more than 15,000 L of liquid carbofuran per year (Otieno et al. 2010). Although carbofuran was banned in 2009 by EPA (Bermúdez-Couso et al. 2011), it is still being used in Africa and Asia perhaps due to its low cost and versatility in agriculture. Recently, Siritham et al. (2013) found 47 µg L⁻¹ of carbofuran in surface water

Responsible editor: Philippe Garrigues

✉ Meththika Vithanage
meththikavithanage@gmail.com

¹ Chemical and Environmental Systems Modeling Research Group, National Institute of Fundamental Studies, Kandy, Sri Lanka

² Korea Biochar Research Center & Department of Biological Environment, Kangwon National University, Chuncheon 200-701, Republic of Korea

³ School of Environmental Sciences, Jawaharlal Nehru University, New Delhi, India

samples collected from vegetable plantation areas. Chowdhury et al. (2012) have found $198.7 \mu\text{g L}^{-1}$ maximum amount of carbofuran at paddy and vegetable fields in Bangladesh. Due to existence of carbofuran at elevated concentrations in several parts of the world, appropriate, cost effective, and environment friendly remediation techniques are continuously in demand. Adsorption is the simplest, most effective, and most widely used technology for most remediation attempts, and activated carbon is the most commonly used adsorbent due to its wide applicability. At the operational mode, adsorption may happen as static (batch) adsorption and dynamic adsorption (Xu et al. 2013). Batch adsorption can be carried out in a closed system with a desired amount of adsorbent, whereas dynamic adsorption occurs in an open system with a continuous flow of adsorbate solution through a column packed with adsorbent.

Biochar (BC), a carbonaceous material produced by limited or no oxygen pyrolysis of biomass, is an emerging efficient adsorbent for the remediation of organic contaminants (Zheng et al. 2010). As BC can be produced from different feedstocks, it has high potential to utilize agricultural and municipal wastes. Approximately 120 of mega tons of rice husk are produced per year worldwide as a by-product of rice harvests. These residues frequently become a waste problem, or they are combusted in an uncontrolled manner causing air pollution, health impacts, and nutrition loss in most of rice cultivation-based countries. Thus, producing BCs is being suggested as a sustainable management option (Masulili et al. 2010). Many researchers have studied the production, characterization, and remediation behaviors of different BCs, and few studies have focused on changing BC properties to increase its efficiency (Azargohar and Dalai 2008; Uchimiyu et al. 2012). Steam activation may cause well-developed and accessible pores to the BC structure and enhance crystalline C formation (Lehmann and Joseph 2009). Recently, it has been reported that surface area and pore volume of BC tend to be increased by steam activation due to the removal of trapped products of incomplete combustion in the process of thermal treatment (Rajapaksha et al. 2014).

Only a little work has been done to examine the relative importance of steam activation on sorption of organic compounds (Rajapaksha et al. 2015; Rajapaksha et al. 2014). To authors' knowledge, no considerable attempt has been made to study the aptitude of steam-activated rice husk biochar on carbofuran removal. Moreover, when considering batch and dynamic adsorption, although the latter one is the main option in practical application; insufficient studies are available to model column dynamics. Hence, we aimed to evaluate the adsorption equilibrium of carbofuran in aqueous phase on steam-activated rice husk biochar as well as column dynamics using different models. In addition, effect of pyrolysis temperature and steam activation on BC properties and sorption capacities were also examined.

Materials and methods

Biochar production and steam activation

Rice husk was obtained from a local rice processing mill in Kandy city, Central province, Sri Lanka. After air drying, rice husk was ground and sieved to $<1.0\text{-mm}$ particle size. Sieved rice husk was placed on ceramic crucibles, covered with lids, and pyrolyzed in a muffle furnace (model P330, Nabertherm, Germany) under limited oxygen conditions. Pyrolysis conditions were set to $7 \text{ }^\circ\text{C min}^{-1}$ until reaching desired peak temperature at 300, 500, and 700 $^\circ\text{C}$. Each pyrolysis temperature was held for 3 h, and produced BCs were allowed to cool down overnight in the furnace. The produced BCs were designated as RHBC300, RHBC500, and RHBC700. For steam activation, portions of RHBC700 were subjected to 5 mL min^{-1} of steam for an additional 45 min under the peak temperature after completing 3 h pyrolysis period. Steam-activated BC was designated as RHBC700S.

Biochar characterization

Proximate analysis was carried out according to the method given elsewhere in order to determine moisture, volatile matter, resident matter, and ash content (Ahmad et al. 2013). A digital pH meter (model 702SM, Metrohm, Switzerland) and electrical conductivity meter (model 5 STAR, Thermo Scientific, Environmental Instruments, USA) were used to determine pH and electrical conductivity (EC), respectively in 1:10 RHBC/water suspension (W/V). Ultimate analysis was done to evaluate elemental composition by using an elemental analyzer (model Vario MAX CN, elemental, Hanau, Germany). Pore characteristics of RHBCs including pore volume and pore diameter were determined by using the Barret-Joyner-Halender (BJH) method from the N_2 adsorption data. Surface morphology was examined by field emission scanning electron microscope (FE-SEM) equipped with an energy dispersive spectrophotometer (model SU8000, Hitachi, Tokyo, Japan). Specific surface areas were determined from adsorption isotherms using Brunauer-Emmett-Teller (BET) equation.

Adsorption edge and batch sorption experiments

The pH value of a solution is crucial for changes in the surface charge of adsorbents, the degree of ionization of the adsorbate, as well as the speciation of the adsorbent (Mamindy-Pajany et al. 2014). The pH effect was studied in aqueous buffer solutions ranging from 3 to 9 using 1 g L^{-1} biochar dosage and 1000 mg L^{-1} stock solution of carbofuran obtained from Sigma Aldrich, USA. The buffer solutions of pH 3–5 were prepared by mixing appropriate volumes of sodium acetate ($0.1 \text{ M CH}_3\text{COONa}$) and acetic acid ($0.1 \text{ M CH}_3\text{COOH}$).

Buffer solutions of pH 7–9 were prepared by mixing aqueous ammonia and phosphoric acid with ammonium phosphate solution (0.1 M (NH₄)₃PO₄). All the solutions were prepared with distilled deionized water (resistivity: 18.2 MΩcm⁻¹). Samples were equilibrated in a mechanical shaker (model EYELA B603) at room temperature (30 °C) for 4 h at 100 rpm. After equilibration, each sample was filtered using a Millipore membrane filter (0.45 μm). The absorbance of the samples was recorded by a double beam UV-Vis spectrophotometer (model UV-160 A, Shimadzu, Japan) at 276 nm, and the remaining carbofuran concentration was determined using a curvilinear calibration obtained in the concentration range 5–100 mg L⁻¹.

Sorption experiments were performed using 1 g L⁻¹ of RHBC dosage using three replicates. A series of carbofuran solutions ranging from 5 to 100 mg L⁻¹ were prepared and buffered at pH 5.0 with acetate buffer. After a 4-h equilibrium period, samples were analyzed for remaining carbofuran concentrations according to above mentioned procedure. The amount of carbofuran adsorbed, *q_e* (mg g⁻¹) was calculated by Eq. 1:

$$q_e = [C_0 - C_e]VM^{-1} \tag{1}$$

where *C_o* and *C_e* are the initial and equilibrium carbofuran aqueous phase concentrations (mg L⁻¹), *V* is the solution volume (L), and *M* is the RHBC mass (g).

Adsorption data modeling

Carbofuran batch sorption data were analyzed using several isotherm models such as Freundlich (Eq. 2), Langmuir (Eq. 3), Temkin (Eq. 5), and Dubinin-Radushkevich (Eq. 6). The model fitting was accomplished by the Origin 6.0 software. Freundlich adsorption isotherm describing adsorption characteristics for the heterogeneous surfaces with different affinities is expressed as,

$$q_{ads} = K_f C_e^n \tag{2}$$

where *q_{ads}* is the amount of carbofuran adsorbed per unit weight of RHBC (mg g⁻¹) and *K_F* and *n* are indicators of adsorption capacity and intensity, respectively. The value of *n* indicates favorability of the adsorption. If *n* = 1, then the partition between the two phases is independent of the concentration, where *n* < 1, it indicates a favorable process and if *n* > 1, the process is not favorable for adsorption. The Langmuir model assumes that all adsorption sites have equal affinity for adsorbate and suggests the monolayer coverage of carbofuran onto RHBC (Foo and Hameed 2010). Langmuir adsorption isotherm is defined as,

$$q_{ads} = \frac{q_{max}K_L C_e}{1 + K_L C_e} \tag{3}$$

Maximum adsorption capacity is denoted by *q_{max}* (mg g⁻¹), and *K_L* is the Langmuir affinity parameter (L mg⁻¹). The essential characteristics of the Langmuir isotherm are expressed in terms of dimensionless separation factor (*R_L*).

$$R_L = \frac{1}{1 + K_L C_0} \tag{4}$$

Langmuir separation factor, *R_L*, indicates the adsorption nature to be either unfavorable (*R_L* > 1), linear (*R_L* = 1), favorable (0 < *R_L* < 1), or irreversible (*R_L* = 0). The Temkin model, related to the heat of sorption, is expressed by Eq. 5. It assumes that the heat of adsorption of all molecules in the layer would decrease linearly rather than logarithmically with increase in coverage of the adsorbent surface and that adsorption is characterized by a uniform distribution of binding energies up to a maximum binding energy (Kundu and Gupta 2006).

$$q_{ads} = \frac{RT}{b} \ln(AC_e) \tag{5}$$

where *R*, *T*, *b*, and *A* represent the universal gas constant (8.314 J K⁻¹ mol⁻¹), absolute temperature (K), heat of adsorption (J), and binding constant (L mg⁻¹), respectively. The Dubinin-Radushkevich model, describing adsorption isotherm in micropores, is given by Eq. 6:

$$q_{ads} = q_D \exp\left(-B_D \left[RT \ln\left(1 + \frac{1}{C_e}\right)\right]^2\right) \tag{6}$$

Where *q_D* is the monolayer adsorption capacity (mg g⁻¹) and *B_D* is the mean free energy of sorption (mol² kJ⁻²). Bonding energy for the ion-exchange mechanism (*E*) can be calculated from the Dubinin-Radushkevich model, using Eq. 7:

$$E = \frac{1}{2B_D^{0.5}} \tag{7}$$

If the magnitude of *E* is between 8 and 16 kJ mol⁻¹, the sorption process is governed by ion exchange, while for values of *E* < 8 kJ mol⁻¹, the sorption process is of a physical nature (Altundogan et al. 2007).

Column experiments

Best adsorbents (RHBC700 and RHBC700S) for carbofuran removal as selected from isotherm studies were screened for the fixed bed study. The fixed bed column was made of Teflon centrifuge tube (5.2 × 2.8 cm ID) containing 66 g of silica sand (50 mesh size) obtained from Naththandiya silica sand mining area, Sri Lanka. The sand was washed with distilled deionized water to remove impurities before packing the columns, and

then it was wet packed into the column. Known quantity from RHBC700 and RHBC700S (0.5 % of sand weight) was placed into the column so that column bed height was 7.5 cm. Fixed inlet concentration of carbofuran (18.29 mg L⁻¹) was pumped downward through the column bed using a cartridge pump (Masterflex L/S, ColeParmer, Model 751,920, USA) at a flow rate of 1 mL min⁻¹. Samples were collected at the column outlet at different time intervals and were analyzed for carbofuran by the double beam UV-Vis spectrophotometer (model UV-160 A, Shimadzu, Japan) at 276 nm.

Column data modeling

The performance of packed beds is explained through the concept of the breakthrough curve. The breakthrough curve shows the loading behavior of carbofuran to be removed from solution in a fixed bed and is usually expressed in terms of normalized concentration defined as the ratio of effluent carbofuran concentration to inlet carbofuran concentration (C_{ef}/C_{in}) as a function of time or volume of effluent for a given bed height (Öztürk and Kavak 2005).

Three models, Thomas, Adams-Bohart, and Yoon-Nelson, were applied to experimental data to analyze the breakthrough curves by linear regression and to predict the column performance for the removal of carbofuran from aqueous solution. Thomas model assumes Langmuir kinetics of adsorption-desorption and no axial dispersion. The linearized form of the Thomas model is as follows (Eq. 8):

$$\ln\left(\frac{C_{in}}{C_{ef}} - 1\right) = \left(\frac{K_{th}mq_0}{Q}\right) - (K_{th}C_{int}) \quad (8)$$

where K_{th} (mL mg⁻¹ min⁻¹) is the Thomas rate constant, q_0 (mg g⁻¹) is predicted adsorption capacity, m is the amount of adsorbent in the column (g), and Q is the influent flow rate (mL min⁻¹). The Adams-Bohart model is based on the assumption that equilibrium is not instant, and the rate of adsorption is proportional to both the adsorbate concentration and residual capacity of the adsorbent. This model can describe the initial part of the breakthrough curve and is expressed as Eq. 9:

$$\ln\left(\frac{C_{ef}}{C_{in}}\right) = (K_{AB}C_{in}t) - K_{AB}N_0\left(\frac{z}{u_0}\right) \quad (9)$$

where K_{AB} is the mass transfer coefficient (L mg⁻¹ min⁻¹), z is the bed height (cm), u_0 (cm min⁻¹) is the superficial velocity, and N_0 is the sorption capacity per unit volume of fixed bed (mg L⁻¹). Yoon-Nelson model expressed by Eq. 10 is less complicated than other models and requires no detailed data of the system. It is based on the assumption that the rate of decrease in the probability of adsorption for each adsorbate molecule is proportional to the probability of adsorbate

adsorption and the probability of adsorbate breakthrough on the adsorbent.

$$\ln\left(\frac{C_{ef}}{C_{in} - C_{ef}}\right) = (k_{YN}t) - \tau k_{YN} \quad (10)$$

Here, τ is the time required for 50 % adsorbate breakthrough (min) and k_{YN} (min⁻¹) is the rate constant.

FTIR investigations

Infrared spectra of both the bare and the carbofuran-adsorbed RHBCs were obtained by a Fourier Transform Infrared Spectrometer (FTIR Nicolet, model 6700, USA) using sample pellets prepared with fused-KBr.

Results and discussion

Biochar characterization

Physicochemical characteristics of RHBCs are presented in Table 1. Increase of pH values with increasing pyrolysis temperature was possibly due to the separation of alkali salts from the organic materials in the feedstock (Ahmad et al. 2012). When pyrolysis temperature increased from 300 to 700 °C, yield content of RHBCs had declined from 52 to 33 %. This may be attributed to the destruction of cellulose, hemicellulose, and combustion of organic materials at high temperatures (Al-Wabel et al. 2013). Further, at higher pyrolysis temperature, more volatiles had been removed, which resulted in less volatile matter and more resident matter in RHBCs. Removal of volatile material with increased pyrolysis temperature had led to a substantial enhancement in ash content. Elemental analysis data showed that carbon (C) content increased while the amounts of O and H decreased with increasing pyrolysis temperature. The increase in C content with the evaluated pyrolysis temperatures may be due to the increase in the degree of carbonization resulting polyaromatic graphene sheets. However, a decrease in O and H contents may be attributed to the breaking of weaker bonds in RHBC structure and removal of water, hydrocarbons, H₂, CO, and CO₂ during carbonization (Ahmad et al. 2013). Molar H/C and O/C ratios were calculated in order to evaluate the aromaticity of RHBC and polarity, respectively. The aromatic ratios sharply decreased with increasing pyrolysis temperature indicating that the aromaticity markedly increased whereas polarity decreased. Furthermore, molar H/C ratio of ≤0.3 indicated highly condensed aromatic ring systems whereas molar H/C ratio of ≥0.7 suggests non-condensed structures (Cely et al. 2014). Hence, it can be assumed that RHBCs may contain condensed aromatic rings in their structures at 700 °C. Changes in BET surface areas, as well as average pore

Table 1 Proximate and ultimate analyses of RHBCs

Sample	RHBC300	RHBC500	RHBC700	RHBC700S
pH	6.24	7.17	9.87	10.12
Proximate analysis				
Yield (%)	52.55	34.91	33.38	–
Moisture (%)	6.78	5.02	3.42	3.03
Mobile matter (%)	68.91	47.69	26.13	15.96
Resident matter (%)	10.67	29.31	31.21	35.39
Ash (%)	13.63	17.98	39.24	45.62
Ultimate analysis				
C ^a (%)	47.71	49.05	50.56	–
H ^a (%)	3.19	2.09	1.29	–
O ^a (%)	24.69	24.84	7.67	–
N ^a (%)	1.10	0.99	0.65	–
Molar H/C	0.75	0.51	0.32	–
Molar O/C	0.38	0.37	0.12	–
Surface area (m ² g ⁻¹)	68.77	169.81	236.74	251.47
Pore volume (cm ³ g ⁻¹)	0.01	0.02	0.05	0.083
Pore diameter (nm)	9.12	5.57	5.29	4.86

^a Ash and moisture free

volumes and pore diameters, also can be obtained from Table 1. When pyrolysis temperature increased, RHBCs had developed pores with dramatically increased surface area. This can be attributed to the generation of porosity resulted by the removal of volatile material. Surface area and pore volume of RHBC had increased after steam activation. All the pore diameter values were within the range of 4–10 nm indicating that mesopores which may play an essential role in many liquid-solid adsorption processes are dominant in RHBCs. However, steam activation had a little influence on the surface area agreeing with recent observations (Rajapaksha et al. 2015).

Adsorption edges

The influence of the solution pH may be critical to change pesticide properties as well as their adsorption behaviors (Memon et al. 2007). As shown in Fig. 1 (a), adsorption was high in the pH range of 3–5 and then gradually decreased. Adsorption amount increased from 11.84 to 13.18 mg g⁻¹ within the pH range of 3–5, in RHBC700S. When pH increased to 9, adsorption decreased again to 11.12 mg g⁻¹. Due to the reason that variations were quite low, carbofuran may effectively adsorb on RHBCs over a wide range of pH. Nevertheless, the maximum adsorption was observed at pH 5 for all types of RHBCs. In acidic medium, carbofuran may be protonated at the amino group or carbonyl oxygen (Mahalakshmi et al. 2007). Hence, electrostatic attractions

between protonated carbofuran molecules and negatively charged RHBC surface may enhance the carbofuran sorption. Increase of pH results in the reduction of neutral and protonated carbofuran molecules, whereas deprotonated molecular form increases, leading to an electrostatic repulsion between the negatively charged biochar surface and carbofuran molecules which may cause a reduction of carbofuran adsorption on RHBCs in alkaline medium.

Adsorption isotherms

Table 2 summarizes the regression coefficients and isotherm parameters obtained from Langmuir, Freundlich, Temkin, and Dubinin-Radushkevich isotherm models at pH 5. It is evident that equilibrium sorption data fitted both Langmuir and Freundlich models with high regression coefficients ($r^2 > 0.9$) (Fig. 1b). The maximum adsorption capacities determined by Langmuir isotherm model were 30.73, 48.75, 132.87, and 160.77 mg g⁻¹ for RHBC300, RHBC500, RHBC700, and RHBC700S, respectively. Adsorption capacity had increased by over 3-fold with increasing pyrolysis temperature from 300 to 700 °C (Fig. 2). It has been reported that BCs produced at high pyrolysis temperatures exhibit high adsorption capacities in removal of organic pollutants (Ahmad et al. 2012). According to our previous study, tea waste-derived biochars had shown a 10.74 mg g⁻¹ of maximum adsorption capacity (Vithanage et al. 2016). Rice straw-activated carbon effectively removed almost 296 mg g⁻¹ of carbofuran (Chang et al. 2011). Further, it has been reported that 0.0073 mg g⁻¹ amount of carbofuran could be adsorbed by soil (Bermúdez-Couso et al. 2011). Among all BCs, RHBC700S showed the highest maximum adsorption capacity. This could be attributed to increased surface area and development of porous structure after steam activation (Rajapaksha et al. 2015). The relationship between initial concentration (C_0) and Langmuir separation factor (R_L) was established in Fig. 1c. Obtained values of R_L for all BCs are less than one and greater than zero indicating favorable adsorption of carbofuran on RHBCs. This was further confirmed by n values obtained from Freundlich equation. Moreover, n values being less than one indicated the heterogeneity of the surface of the RHBCs. For all RHBCs, calculated E values from Dubinin-Radushkevich model were greater than 35.8 kJ mol⁻¹ (Table 2) suggesting that the adsorption process is more inclined towards chemisorption.

Isotherm data revealed that the adsorption process could be described well by both Freundlich and Langmuir isotherms indicating involvement of both physisorption and chemisorption. However, the r^2 values of each sample of RHBC are higher with Freundlich model than those with Langmuir model indicating that the Freundlich model gives a more satisfactory fitting to adsorption data (Table 2). Data fitting into Freundlich indicates multilayer adsorption. Previously published studies also have

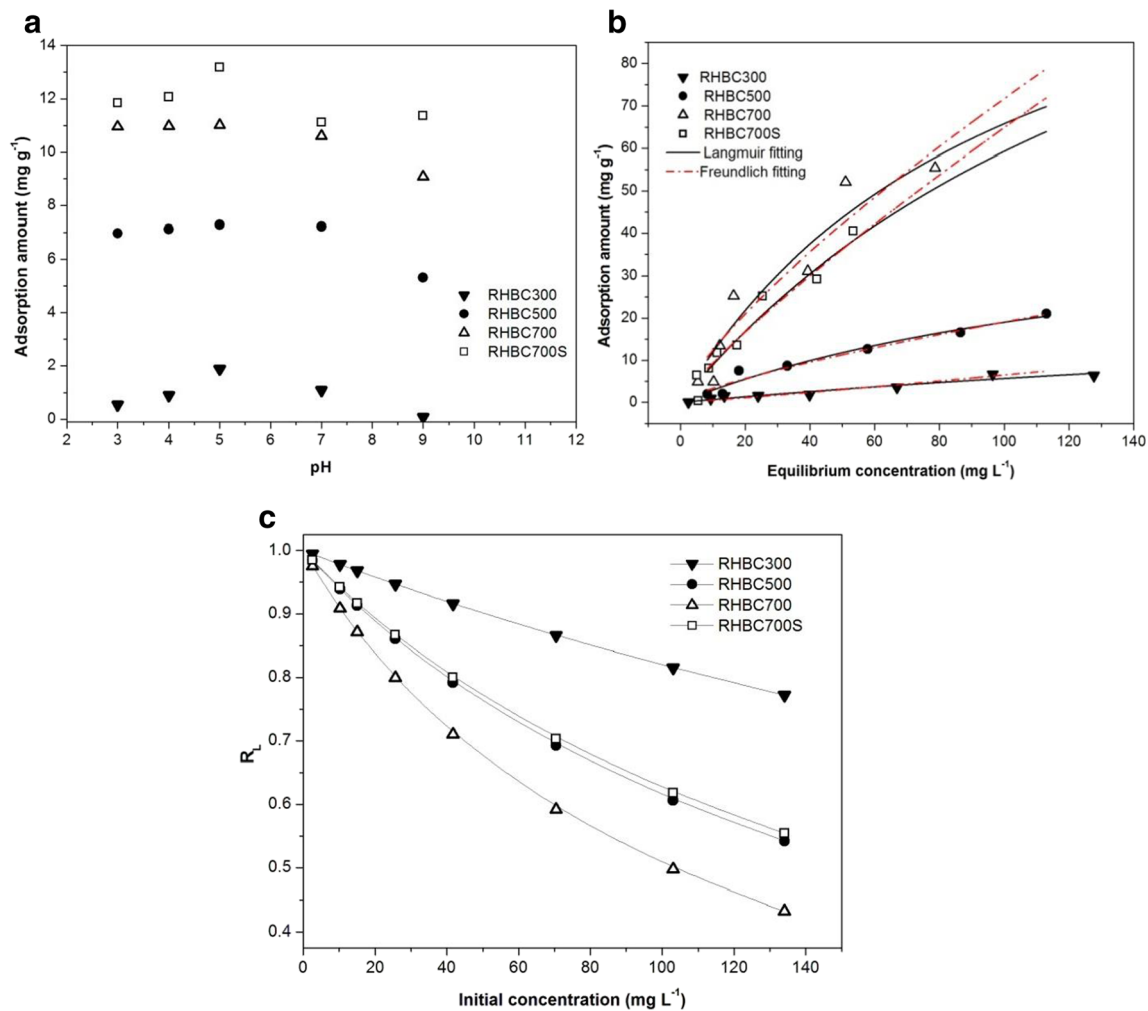


Fig. 1 **a** Adsorption capacity variation with pH. **b** Adsorption isotherm fittings to Langmuir and Freundlich isotherms. The *symbols* represent experimental results at pH 5, and the *solid line* represents the calculated

results using non-linear least square fit. **c** Langmuir separation factors for RHBCs at pH = 5

reported that the Freundlich equation is highly applicable to describe the adsorption of organic contaminants onto BCs (Rajapaksha et al. 2015; Rajapaksha et al. 2014; Zheng et al. 2010). Thus, it can be suggested that the adsorption of carbofuran is a favorable process governed by both physisorption and chemisorption interactions that occur between carbofuran molecules and heterogeneous RHBC surface.

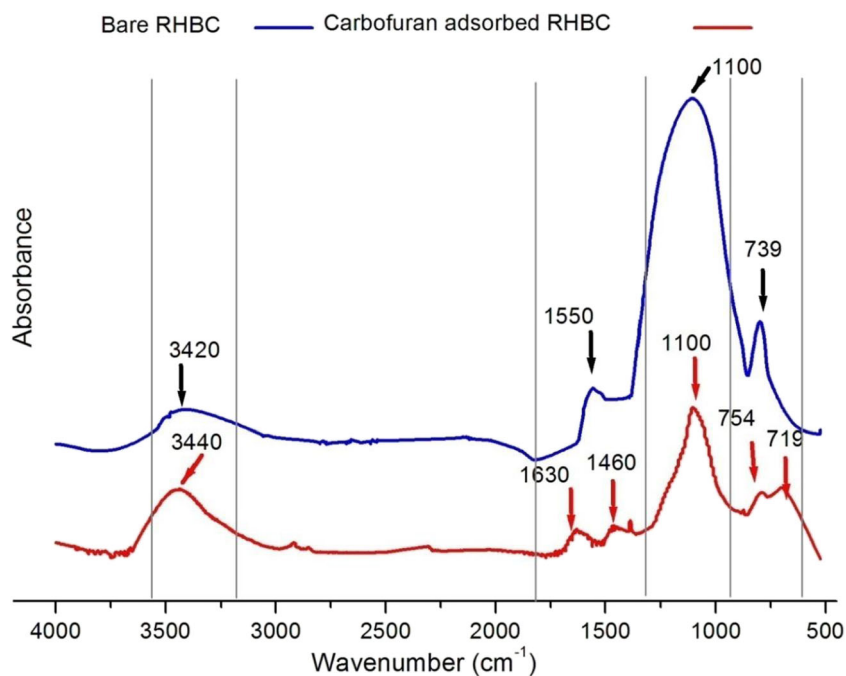
FTIR investigations

Adsorption phenomena could be further elucidated by FTIR spectra of RHBC before and after carbofuran adsorption (Fig. 2). It has been reported that positional fluctuations of FTIR peaks are due to electrostatic and chemical adsorption (Dolphen and Thiravetyan 2011). Broad peaks at 3420 cm^{-1}

Table 2 Langmuir, Freundlich, Temkin, and Dubinin-Radushkevish isotherm parameters for carbofuran adsorption onto RHBCs at pH 5. All parameters were calculated by non-linear regression

Adsorbent	Langmuir			Freundlich			Temkin			Dubinin-Radushkevish			
	q_{max} (mg g^{-1})	K_L (L g^{-1})	r^2	K_F (mg g^{-1})	n	r^2	A (Lmg^{-1})	b	r^2	q_D (mg g^{-1})	B_D ($\text{mol}^2\text{kJ}^{-1}$)	E (kJ mol^{-1})	r^2
RHBC300	30.73	0.0022	0.936	0.104	0.951	0.937	0.206	1506	0.773	7.57	0.00039	35.80	0.845
RHBC500	48.75	0.0063	0.965	0.583	0.756	0.967	0.129	352	0.945	17.56	0.00007	84.51	0.852
RHBC700	132.87	0.0098	0.908	2.110	0.764	0.927	0.175	120	0.912	51.49	0.00004	111.80	0.896
RHBC700S	160.77	0.0060	0.951	1.217	0.843	0.953	0.209	169	0.922	36.46	0.00003	129.09	0.871

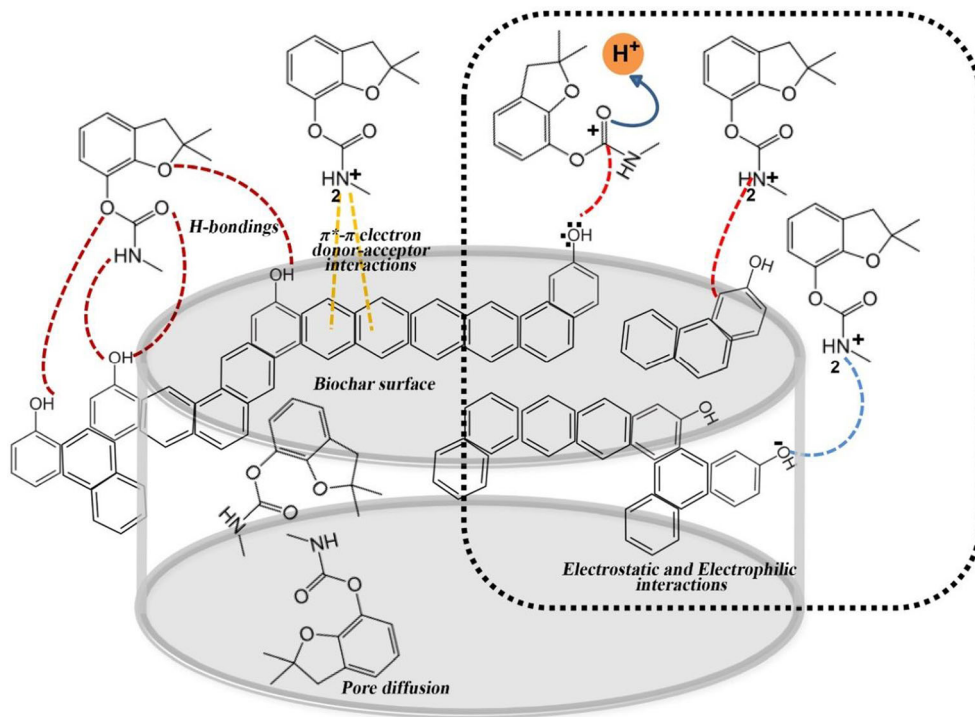
Fig. 2 FTIR spectra of bare and carbofuran adsorbed RHBC700S



in bare RHBC correspond to the vibrations of OH-bonded groups (Chen et al. 2012). This peak has apparently shifted to 3440 cm^{-1} in pesticide-treated RHBC, suggesting that the involvement of alcohols, phenols, and carboxylic acid groups in carbofuran adsorption via hydrogen bonding or dipole-dipole interactions (Ryu et al. 2010). Formation of hydrogen bonds could be further explained by the appearance of a new

peak at 1630 cm^{-1} which is attributed to the H-O-H bending in carbofuran adsorbed RHBC. The band at 1550 cm^{-1} in bare RHBC is ascribed to asymmetric vibrations of O-C-O group (Sahoo et al. 2012). Due to the disappearance of this peak in carbofuran-treated RHBC; it can be proposed that dissociation of such bonds occurs in carbofuran adsorption mechanism. Moreover, C-N bond stretching vibration at 1460 cm^{-1} has

Fig. 3 A graphical representation of possible mechanisms for carbofuran adsorption onto RHBC



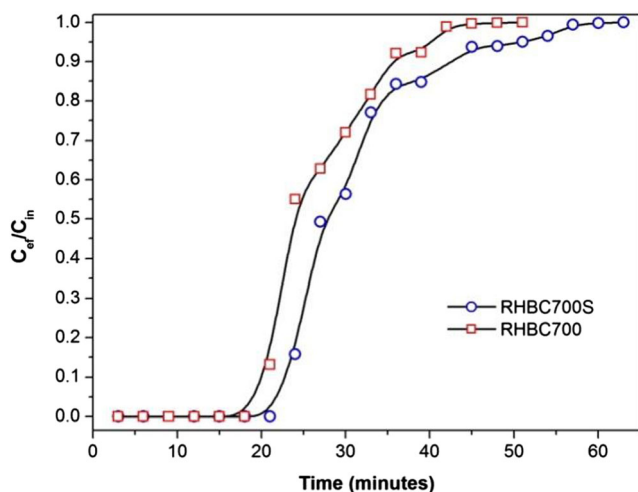


Fig. 4 Breakthrough curves for adsorption of carbofuran onto RHBC700S and RHBC700 (flow rate 1 mL min⁻¹, pH 5)

newly appeared in carbofuran-adsorbed RHBC implying the formation of complexes between carbofuran and RHBC. The characteristic peak, centered at 739 cm⁻¹ in bare RHBC, has been split into two new peaks at 754 and 719 cm⁻¹ after carbofuran adsorption, indicating π^* - π electron donor-acceptor interactions between the adsorbent and pesticide molecules (Shih and Wu 2004). Overall, FTIR results suggest both chemisorptive and physisorptive nature of carbofuran adsorption on RHBCs, exhibiting the involvement of different surface functional groups (Fig. 3). A graphical representation of possible chemisorption and physisorption mechanisms for carbofuran adsorption onto RHBC is illustrated in Fig. 3.

Column adsorption

Breakthrough curves of RHBC700 and RHBC700S for carbofuran adsorption are illustrated in Fig. 4. The fixed bed column with RHBC700 was exhausted faster, and breakthrough point was achieved earlier than fixed bed with RHBC700S. Column bed with RHBC700S exhibited an

Table 3 Thomas, Adams-Bohart, and Yoon-Nelson model parameters for RHBC700 and RHBC700S

Model	Parameters	RHBC700S	RHBC700
Thomas	K_{th} (mL mg ⁻¹ min ⁻¹)	0.006	0.012
	q_0 (mg g ⁻¹)	1401	1226
	r^2	0.975	0.943
Adams-Bohart	K_{AB} (L mg ⁻¹ min ⁻¹)	0.004	0.004
	N_0 (mg L ⁻¹)	7.140	5.899
	r^2	0.912	0.847
Yoon-Nelson	k_{YN} (min ⁻¹)	0.110	0.230
	(min)	26	23
	r^2	0.975	0.942

extended breakthrough curve indicating the potential of treating a higher volume of carbofuran solution. Estimated model parameters are depicted in Table 3. For both adsorbents, the experimental data was well fitted with the Thomas model ($r^2 = 0.975$ and 0.943 for RHBC700S and RHBC700, respectively) and similarly with Yoon-Nelson model. Relatively low r^2 values (0.912 and 0.847 for RHBC700S and RHBC700, respectively) indicated the less applicability of Adams-Bohart model. Hence, the Langmuir kinetics can be applied to explain the carbofuran adsorption by RHBCs in a fixed bed system rather than external and internal diffusion (Rao and Viraraghavan 2002). The predicted maximum adsorption capacity of RHBC700S (1401 mg g⁻¹) was higher than that of RHBC700 (1226 mg g⁻¹). Higher value of Thomas rate constant K_{th} for RHBC700 (0.012 mL mg⁻¹ min⁻¹) compared to RHBC700S (0.006 mL mg⁻¹ min⁻¹) suggested that internal diffusion in RHBC700 was higher than that in RHBC700S. As obtained from Yoon-Nelson model, the time required for 50 % adsorbate breakthrough (τ) for RHBC700S (26 min) is higher than RHBC700 (23 min). This can be explained by higher probability of adsorption for each molecule to the adsorbate is higher for RHBC700S.

Conclusions

Pyrolysis temperature strongly influenced the physicochemical properties and adsorption capacities of RHBCs. Steam activation could increase carbofuran removal further. The highest adsorption capacity of 160.77 mg g⁻¹ was observed in RHBC700S at pH 5. Carbofuran could be effectively adsorbed onto RHBCs in a wide range of pH. Although the adsorption data fitted well with both Freundlich and Langmuir isotherm models, yet the best fitted model was seemed to be Freundlich isotherm model. It can be concluded that both physical and chemical interactions can govern the adsorption process to heterogeneous RHBC surface. FTIR analyses further suggested the possibility of chemical interactions between adsorbent and the pesticide molecules indicating the contribution from different functional groups. In column adsorption, the breakthrough curves for carbofuran were well predicted by Thomas and Yoon-Nelson models. Thus, dynamic adsorption rate could be described by Langmuir kinetics. Column bed with RHBC700S was capable of treating a higher volume of carbofuran. Hence, it can be concluded that steam-activated RHBC is efficient in the removal of carbofuran in batch as well as fixed bed sorption systems.

Acknowledgments This study is supported by MTR/TRD/AGR/3/1/8, Indo-Sri Lanka bilateral research grant sanctioned by the Ministry of Technology, Research and Atomic Energy, Sri Lanka and the Department of Science and Technology (DST), Government of India.

References

- Ahmad M, Lee SS, Dou X, Mohan D, Sung J-K, Yang JE, Ok YS (2012) Effects of pyrolysis temperature on soybean stover-and peanut shell-derived biochar properties and TCE adsorption in water. *Bioresour Technol* 118:536–544
- Ahmad M et al. (2013) Trichloroethylene adsorption by pine needle biochars produced at various pyrolysis temperatures. *Bioresour Technol* 143:615–622
- Altundogan HS, Arslan NE, Tumen F (2007) Copper removal from aqueous solutions by sugar beet pulp treated by NaOH and citric acid. *J Hazard Mater* 149:432–439
- Al-Wabel MI, Al-Omran A, El-Naggar AH, Nadeem M, Usman AR (2013) Pyrolysis temperature induced changes in characteristics and chemical composition of biochar produced from conocarpus wastes. *Bioresour Technol* 131:374–379
- Azargohar R, Dalai A (2008) Steam and KOH activation of biochar: experimental and modeling studies. *Microporous Mesoporous Mater* 110:413–421
- Bermúdez-Couso A, Fernández-Calviño D, Pateiro-Moure M, Nóvoa-Muñoz JC, Simal-Gándara J, Arias-Estévez M (2011) Adsorption and desorption kinetics of carbofuran in acid soils. *J Hazard Mater* 190:159–167
- Cely P, Tarquis A, Paz-Ferreiro J, Méndez A, Gascó G (2014) Factors driving the carbon mineralization priming effect in a sandy loam soil amended with different types of biochar. *Solid Earth* 5:585–594
- Chang K-L, Lin J-H, Chen S-T (2011) Adsorption studies on the removal of pesticides (Carbofuran) using activated carbon from rice straw agricultural waste. *World Acad Sci Eng Technol* 76:348–351
- Chen J-q, Hu Z-j, Ji R (2012) Removal of carbofuran from aqueous solution by orange peel. *Desalin Water Treat* 49:106–114
- Chowdhury MAZ, Banik S, Uddin B, Moniruzzaman M, Karim N, Gan SH (2012) Organophosphorus and carbamate pesticide residues detected in water samples collected from paddy and vegetable fields of the Savar and Dhamrai Upazilas in Bangladesh. *Int J Environ Res Public Health* 9:3318–3329
- DeZuane J (1997) *Handbook of drinking water quality*. John Wiley & Sons, New York
- Dolphin R, Thiravetyan P (2011) Adsorption of melanoidins by chitin nanofibers. *Chem Eng J* 166:890–895
- Foo K, Hameed BH (2010) An overview of dye removal via activated carbon adsorption process. *Desalin Water Treat* 19:255–274
- Kundu S, Gupta A (2006) Arsenic adsorption onto iron oxide-coated cement (IOCC): regression analysis of equilibrium data with several isotherm models and their optimization. *Chem Eng J* 122:93–106
- Lehmann J, Joseph S (2009) *Biochar for environmental management: science and technology*. Earthscan, London
- Mahalakshmi M, Arabindoo B, Palanichamy M, Murugesan V (2007) Photocatalytic degradation of carbofuran using semiconductor oxides. *J Hazard Mater* 143:240–245
- Makehelwala M, Weerasooriya R, Jayaratne L, Dissanayake C (2012) Thermodynamics of carbofuran adsorption on pyrite. *J Chem Thermodyn* 51:1–7
- Mamindy-Pajany Y, Sayen S, Mosselmans JFW, Guillon E (2014) Copper, nickel and zinc speciation in a biosolid-amended soil: pH adsorption edge, μ -XRF and μ -XANES investigations. *Environ Sci Technol* 48:7237–7244
- Masullili A, Utomo WH, Syechfani M (2010) Rice husk biochar for rice based cropping system in acid soil I. The characteristics of rice husk biochar and its influence on the properties of acid sulfate soils and rice growth in West Kalimantan, Indonesia. *J Agric Sci* 2:39
- Memon GZ, Bhangar M, Akhtar M (2007) The removal efficiency of chestnut shells for selected pesticides from aqueous solutions. *J Colloid Interface Sci* 315:33–40
- Otieno PO, Lalah JO, Virani M, Jondiko IO, Schramm K-W (2010) Carbofuran and its toxic metabolites provide forensic evidence for Furadan exposure in vultures (*Gyps africanus*) in Kenya. *Bull Environ Contam Toxicol* 84:536–544
- Öztürk N, Kavak D (2005) Adsorption of boron from aqueous solutions using fly ash: batch and column studies. *J Hazard Mater* 127:81–88
- Rajapaksha AU, Vithanage M, Zhang M, Ahmad M, Mohan D, Chang SX, Ok YS (2014) Pyrolysis condition affected sulfamethazine sorption by tea waste biochars. *Bioresour Technol* 166:303–308
- Rajapaksha AU et al. (2015) Enhanced sulfamethazine removal by steam-activated invasive plant-derived biochar. *J Hazard Mater* 290:43–50
- Rao J, Viraraghavan T (2002) Biosorption of phenol from an aqueous solution by *Aspergillus Niger* biomass. *Bioresour Technol* 85:165–171
- Remya N, Lin J-G (2011) Microwave-assisted carbofuran degradation in the presence of GAC, ZVI and H₂O₂: influence of reaction temperature and pH. *Sep Purif Technol* 76:244–252
- Ryu SR, Noda I, Jung YM (2010) What is the origin of positional fluctuation of spectral features: true frequency shift or relative intensity changes of two overlapped bands? *Appl Spectrosc* 64:1017–1021
- Sahoo S, Chakraborti C, Behera P, Mishra S (2012) FTIR and Raman spectroscopic investigations of a Norfloxacin/Carbopol934 Polymeric suspension. *Journal of Young Pharmacists* 4:138–145
- Salman J, Hameed B (2010) Adsorption of 2, 4-dichlorophenoxyacetic acid and carbofuran pesticides onto granular activated carbon. *Desalination* 256:129–135
- Shackley S et al. (2012) Sustainable gasification–biochar systems? A case-study of rice-husk gasification in Cambodia, part I: context, chemical properties, environmental and health and safety issues. *Energy Policy* 42:49–58
- Shih YH, Wu SC (2004) Kinetics of toluene sorption and desorption in Ca- and Cu-montmorillonites investigated with Fourier transform infrared spectroscopy under two different levels of humidity. *Environ Toxicol Chem* 23:2061–2067
- Siritham C, Thammakhet C, Thavarungkul P, Kanatharana P (2013) Online microchannel preconcentrator for carbofuran detection. *Journal of Environmental Science and Health, Part B* 48:893–905
- Uchimiya M, Bannon DI, Wartelle LH (2012) Retention of heavy metals by carboxyl functional groups of biochars in small arms range soil. *J Agric Food Chem* 60:1798–1809
- Vithanage M, Mayakaduwa S, Herath I, Ok YS, Mohan D (2016) Kinetics, thermodynamics and mechanistic studies of carbofuran removal using biochars from tea waste and rice husks. *Chemosphere* 150:781–789
- WHO (2006) *The world health report: 2006: working together for health*. World Health Organization, Geneva
- Xu Z, Cai J-g, Pan B-c (2013) Mathematically modeling fixed-bed adsorption in aqueous systems. *Journal of Zhejiang University Science A* 14:155–176
- Zheng W, Guo M, Chow T, Bennett DN, Rajagopalan N (2010) Sorption properties of greenwaste biochar for two triazine pesticides. *J Hazard Mater* 181:121–126